Simulation of the Fuel Isotope Effect on the Confinement Property in DT Fusion Reactors*)

Tetsutarou OISHI, Kozo YAMAZAKI, Yoshihito HORI and Hideki ARIMOTO

Nagoya University, Furo-cho, Chikusa-ku, Nagoya 464-8603, Japan

(Received 8 December 2010 / Accepted 31 March 2011)

To sustain deuterium (D) - tritium (T) burning plasmas efficiently and to reduce T fuel injection into magnetic confinement fusion reactors, the amount and the ratio of D and T both in the bulk plasmas and in the fueling systems should be controlled accurately. In order to analyze the relationship among fueling methods, the D/T fuel ratio, and reactor output power numerically, we applied the toroidal transport analysis linkage (TOTAL) equilibrium-transport integrated simulation code to model the fuel supply in D-T burning plasmas. It was revealed that operation with a lower tritium ratio in the fuel pellet and a higher electron density can reduce the T fuel injection. The isotope effect of the ion mass on the confinement property was also investigated. As a preliminary result, a concern emerged that the improved confinement of helium ions causes an unintended increase of the electron density, if the particle diffusion coefficient of the ions has a negative correlation with the ion mass.

Keywords: tokamak, D/T fuel ratio, burning plasma, pellet injection, tritium consumption, transport analysis, integrated simulation code, isotope effect

DOI: 10.1585/pfr.6.2401052

1. Introduction

To sustain deuterium (D) - tritium (T) burning plasmas efficiently in magnetic confinement fusion reactors, the amount and the ratio of D and T to be supplied into the reactor as fuels should be controlled optimally. For the more accurate evaluation and control of the D/T ratio, the isotope effect of the bulk ion on the transport should be investigated. Indeed, the dependency of the energy confinement time τ_e on the average mass number $<A>$ in D-T experiments has been demonstrated at JET and TFTR [1,2]. This indicates that the confinement is improved in the tritium-rich plasmas. On the other hand, from the viewpoint of reactor engineering, the tritium consumption should not be too large because of its radioactivity and scarcity. Therefore, it is important to optimize the reactor operation to both achieve good performance and conserve the tritium resource.

In the present study, the relationship among D/T fuel ratio, tritium consumption, and output reactor power in the D-T burning plasmas in a tokamak reactor is analyzed numerically using the TOTAL (toroidal transport analysis linkage) equilibrium-transport integrated simulation code [3]. We focus on the following two topics in the present paper:

- Proposal of a reactor operation scenario with reduced tritium consumption.
- Investigation of the effect of the isotope in transport on the tritium consumption.

author's e-mail: t-oishi@mail.nucl.nagoya-u.ac.jp

*) This article is based on the presentation at the 20th International Toki Conference (ITC20).

2. Simulation Methods

We applied the TOTAL code to model the fuel supply in the D-T burning plasmas. The TOTAL code combines on the one hand, the 2-dimensional equilibrium code APOLLO [4] or 3-dimensional equilibrium code VMEC [5] to calculate the equilibrium of a tokamak or helical magnetic configuration, respectively, and on the other, the 1-dimensional transport simulation code to calculate the radial profile of plasma parameters. Different models of fuel supply, such as pellet injection, neutral beam injection or gas puffing, can be included in the code.

In the transport calculation, the thermal diffusion coefficient χ is determined as

$$\chi = \chi_{\mathrm{NC}} + \chi_{\mathrm{AN}} \times F(\omega_{E\times B}/\gamma_{\mathrm{ITG}}), \tag{1}$$

where χ_{NC} and χ_{AN} are the neoclassical and anomalous thermal diffusion coefficients, respectively. The Bohm and Gyro-Bohm mixed model [6] is employed to express χ_{AN},

$$\chi_{\mathrm{AN}} = 4.0\chi_{\mathrm{Bohm}} + 0.5\chi_{\mathrm{Gyro\text{-}Bohm}}, \tag{2}$$

$$\chi_{\mathrm{Bohm}} = 4\times 10^{-5} R \left|\frac{\nabla(n_e T_e)}{n_e B_\phi}\right| q^2, \tag{3}$$

$$\chi_{\mathrm{Gyro\text{-}Bohm}} = 5\times 10^{-6} \sqrt{T_e} \left|\frac{\nabla T_e}{B_\phi^2}\right|. \tag{4}$$

We have employed a transport model considering the suppression of turbulence by $E\times B$ shear and the resulting improvement of confinement [7]. This model focuses on the ion temperature gradient (ITG) mode [8] as the representative turbulence. $F(\omega_{E\times B}/\gamma_{\mathrm{ITG}})$ in Eq. (1) is the improvement factor [9] defined as

$$F(\omega_{E\times B}/\gamma_{\rm ITG}) = \frac{1}{1+(\tau\,\omega_{E\times B}/\gamma_{\rm ITG})^{\gamma}}. \quad (5)$$

$\omega_{E\times B}$ is the $E\times B$ flow shearing rate [10] defined as

$$\omega_{E\times B} = \left|\frac{RB_\theta}{B_\phi}\frac{\partial}{\partial r}\left(\frac{E_r}{RB_\theta}\right)\right|, \quad (6)$$

where the radial electric field E_r is calculated using an approximation formula:

$$\frac{{\rm d}E_r}{{\rm d}r} = -\frac{1}{n_{\rm i}^2}\frac{{\rm d}n_{\rm i}}{{\rm d}r}\frac{{\rm d}p_{\rm i}}{{\rm d}r}. \quad (7)$$

In this formula, E_r is calculated by considering the radial force balance, and the toroidal and poloidal ion flows are assumed to be small [11]. $\gamma_{\rm ITG}$ is the linear growth rate of the ITG mode defined as

$$\gamma_{\rm ITG} = \frac{(\eta_{\rm i}-2/3)^{1/2}\,|s|\,c_{\rm i}}{qR}, \quad s = \frac{r}{q}\left(\frac{{\rm d}q}{{\rm d}r}\right), \quad (8)$$

where $\eta_{\rm i} = L_{\rm n}/L_T$ is the ratio between the ion density scale length $L_{\rm n}$ and the ion temperature scale length L_T, s is the magnetic shear, and $c_{\rm i} = (T_{\rm i}/m_{\rm i})^{1/2}$ [8]. The particle diffusion coefficient D is determined as $D = D_{\rm NC} + D_{\rm AN}$, where $D_{\rm NC}$ and $D_{\rm AN}$ are the neoclassical and anomalous particle diffusion coefficients, respectively. The anomalous part of the particle diffusion coefficient $D_{\rm AN}$ is calculated as $D_{\rm AN} = (0.3+0.7\rho)\,\chi_{\rm eAN}\chi_{\rm iAN}/(\chi_{\rm eAN}+\chi_{\rm iAN})$.

Each proportional coefficient for $\chi_{\rm Bohm}$ and $\chi_{\rm Gyro\text{-}Bohm}$ in Eq. (2), parameters τ and γ in Eq. (5) ($\tau = 2.0$ and $\gamma = 4.0$), and the model of $D_{\rm AN}$ stated above were determined by comparison with the experimental data of the reversed shear discharge with ITB of the JT-60U tokamak (#29728, #32423) [12]. Using Eqs. (1-5), we assumed that the anomalous transport is suppressed when $\omega_{E\times B}$ exceeds $\gamma_{\rm ITG}$. As stated in the previous section, the confinement tended to improve in the tritium-rich plasmas in the D-T experiments. To include this effect in our simulation model, the dependency of the particle diffusion coefficient $D_{\rm i}$ on the ion mass $m_{\rm i}$ for the ion species i is assumed as

$$D_{\rm i} = D(m_{\rm i}/m_{\rm D})^{-x}, \quad {\rm i} = {\rm D, T, ^4He}, \quad x > 0. \quad (9)$$

The plasma parameters of an ITER-like tokamak reactor with reversed shear configuration as a simulation target were determined using the reactor design system PEC (Physics-Engineering-Cost) code [13]. The main plasma parameters were as follows: major radius $R_{\rm p} = 5.29$ m, minor radius $a_{\rm p} = 1.25$ m, toroidal field $B_{\rm z0} = 7.11$ m, plasma current $I_{\rm p} = 13.0$ MA, alpha-heating power = 600.0 MW, ellipticity = 2.0, and triangularity = 0.5. These parameters refer to the 1GW electric power generated by the D-T reaction.

The "neutral gas shielding (NGS) model" [14] gives the ablation rate along the pellet path l as

$$\frac{{\rm d}N}{{\rm d}l} = 4.38\times10^3 N^{0.444} n_{\rm e}^{0.333} T_{\rm e}^{1.64} M_{\rm i}^{-0.333}/V_{\rm p}, \quad (10)$$

where N is the number of atoms in a pellet, $M_{\rm i}$ is the pellet mass, and $V_{\rm p}$ is the pellet injection velocity.

It is widely recognized that the pellet injection from the high-field-side (HFS) is effective for injecting pellets deep into the core region of the tokamak plasma [15]. To simulate HFS pellet injection in tokamaks, we applied the "mass relocation model" [16], which describes the plasmoid drift generated by pellet ablation.

3. Simulation Results

Figure 1 shows the simulation results of temporal evolutions of plasma parameters in the reversed shear tokamak reactor with fueling by pellet injection. The alpha heating power P_α, auxiliary heating power $P_{\rm aux}$, and radiation power loss $P_{\rm rad}$ are shown in Fig. 1 (a). In this simulation, both the pellet injection frequency and the auxiliary heating power are feedback-controlled such that the alpha particle heating power increases linearly in the initial state (< 50 sec). The pellet injection frequency is also controlled during the steady self-burning state (> 50 sec) such that the alpha particle heating power is kept at a target value. Figures 1 (b-d) show the average electron density $<n_{\rm e}>$, electron temperature $<T_{\rm e}>$, and ion temperature $<T_{\rm i}>$, β value, normalized β value $\beta_{\rm N}$, energy confinement time $\tau_{\rm e}$ calculated in this code and evaluated from IPB98(y,2) scaling, and improvement factor $H_{\rm H98y2}$. These

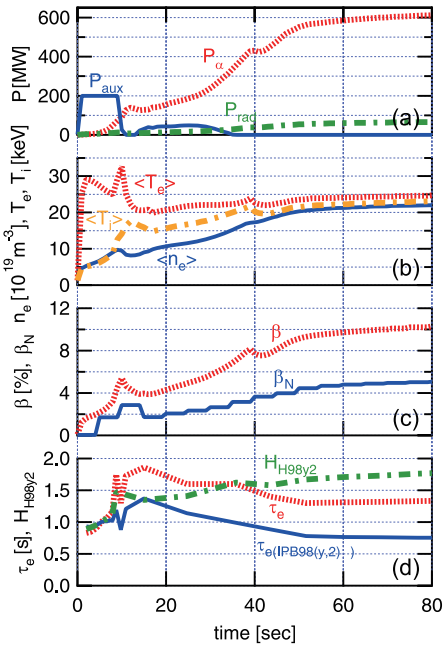

Fig. 1 Simulation results of temporal evolutions in the reversed shear tokamak reactor with fueling by pellet injection. (a) Alpha heating power P_α, auxiliary heating power $P_{\rm aux}$, radiation power loss $P_{\rm rad}$. (b) Average electron density $<n_{\rm e}>$, electron temperature $<T_{\rm e}>$, and ion temperature $<T_{\rm i}>$. (c) β value and normalized β value $\beta_{\rm N}$. (d) Energy confinement time $\tau_{\rm e}$ calculated in this code and evaluated from IPB98(y,2) scaling, and improvement factor $H_{\rm H98y2}$.

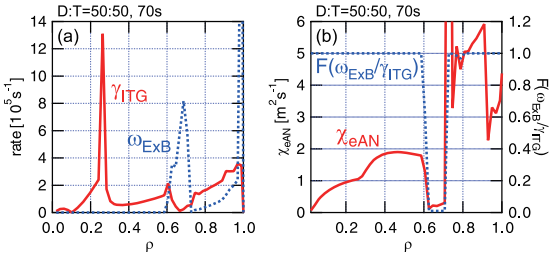

Fig. 2 Radial profiles of (a) the linear growth rate of the ITG mode γ_{ITG} and the $E\times B$ shearing rate $\omega_{E\times B}$, (b) the improvement factor $F(\omega_{E\times B}/\gamma_{ITG})$ and the anomalous electron thermal diffusion coefficient χ_{eAN}.

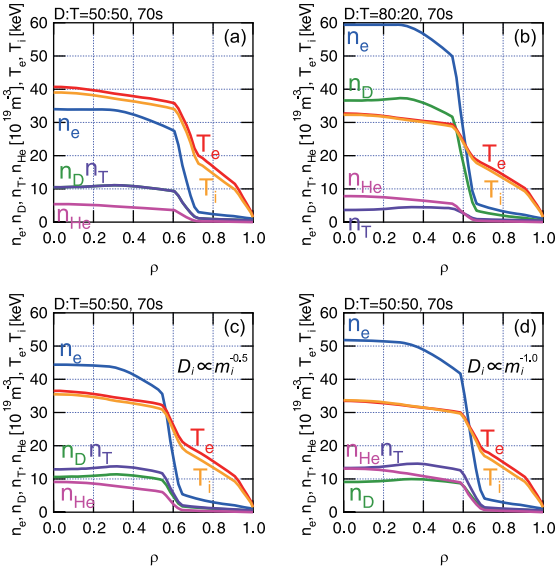

Fig. 3 Radial profiles of electron temperature T_e, ion temperature T_i, electron density n_e, deuterium ion density n_D, tritium ion density n_T, and He^{2+} ion density n_{He} in the steady self-burning state. The D/T ratios in the pellets were (a) 50/50 and (b) 80/20. Dependency of the particle diffusion coefficient D_i on the ion mass m_i is assumed as (c) $D_i \propto m_i^{-0.5}$ and (d) $D_i \propto m_i^{-1.0}$. In (c) and (d), the D/T ratio in the pellets is 50/50.

parameters shown in Fig. 1 were obtained from the simulation using a fuel pellet consisting of 50% deuterium and 50% tritium.

The radial profiles of the simulation results that are related to the improvement of the confinement are shown in Fig. 2. These parameters are obtained in the steady self-burning state of the simulation shown in Fig. 1. The linear growth rate of the ITG mode γ_{ITG} exceeds the $E\times B$ shearing rate $\omega_{E\times B}$ at the normalized radius ρ of 0.6-0.7, as shown in Fig. 2 (a). Then, the improvement factor $F(\omega_{E\times B}/\gamma_{ITG})$ defined in Eq. (5) becomes close to zero at the corresponding normalized radius, resulting in the suppression of the anomalous electron thermal diffusion coefficient χ_{eAN}, as shown in Fig. 2 (b).

Figure 3 shows the radial profiles of electron temperature T_e, ion temperature T_i, electron density n_e, deuterium ion density n_D, tritium ion density n_T, and He^{2+} ion density n_{He} in the steady self-burning state. The D/T ratio in the pellets has definite effects on electron density and transport properties. The results for D/T pellet ratios of 50/50 and 80/20 are shown in Figs. 3 (a) and 3 (b), respectively. The density profiles of deuterium and tritium are identical in Fig. 3 (a), while they are quite different in Fig. 3 (b). In the case in Fig. 3 (b), the short supply of tritium is compensated by increasing the deuterium. The electron density in Fig. 3 (b) should be larger than that in Fig. 3 (a) because the production of n_D and n_T, which is proportional to the target alpha heating power, would be the same in these two cases. On the other hand, the dependency of the particle diffusion coefficient D_i on the ion mass m_i as stated in Eq. (9) is assumed as $D_i \propto m_i^{-0.5}$ in Fig. 3 (c) and $D_i \propto m_i^{-1.0}$ in Fig. 3 (d). In Figs. 3 (c) and 3 (d), the D/T ratio in the pellet is 50/50. In the case with larger dependency, the tritium density becomes larger than the deuterium density. In addition, the He^{2+} density also increases, which results in the necessity of increased electron density.

From the analysis stated above, it is clarified that the operation regime of density and temperature in the steady self-burning state varies with the D/T ratio in the pellet and the dependency of the transport property on the ion mass. The frequency of the pellet injection f_{pel}, which is defined by the number of pellets to be injected to the reactor per unit time, is also varied to sustain the burning plasma at the target alpha heating power. Then, we can evaluate the tritium consumption per unit time $N_{T(atom)}$ by multiplying the pellet frequency and the tritium ratio in the pellet for each tritium ratio. Figure 4 shows the average electron density $<n_e>$, electron temperature $<T_e>$, ion temperature $<T_i>$, as well as f_{pel} and $N_{T(atom)}$, plotted against the tritium ratio in the pellet. The dependency of D_i on m_i is not assumed in Figs. 4 (a) and 4 (b). As the D/T ratio becomes asymmetrical, higher density is required and the temperature decreases. We have to notice that the density exceeds the Greenwald density limit in the case that the tritium ratio is extremely small. In the result in Figs. 4 (a) and 4 (b), a tritium ratio larger than 30% is an available operation regime from the viewpoint of the density limit. One can see that the minimum value of $N_{T(atom)}$ in the available operation regime is 28% smaller than that with D/T ratio in the pellet of 50/50. On the other hand, the dependency of D_i on m_i is assumed as $D_i \propto m_i^{-0.5}$ in Figs. 4 (c) and 4 (d). Compared to Figs. 4 (a) and 4 (b), the increased average density makes the available operation regime below the density limit narrower. The reduction of $N_{T(atom)}$ is limited to only a few percent. In addition, $D_i \propto m_i^{-1.0}$ is assumed in Figs. 4 (e) and 4 (f). The results in these figures indicate that we have no operation regime for the D/T ratio in the pellet because the electron density is increased too much due to the improved confinement of He ions. In this case, effective exhaust of the helium ash is needed to suppress the increase of the electron density.

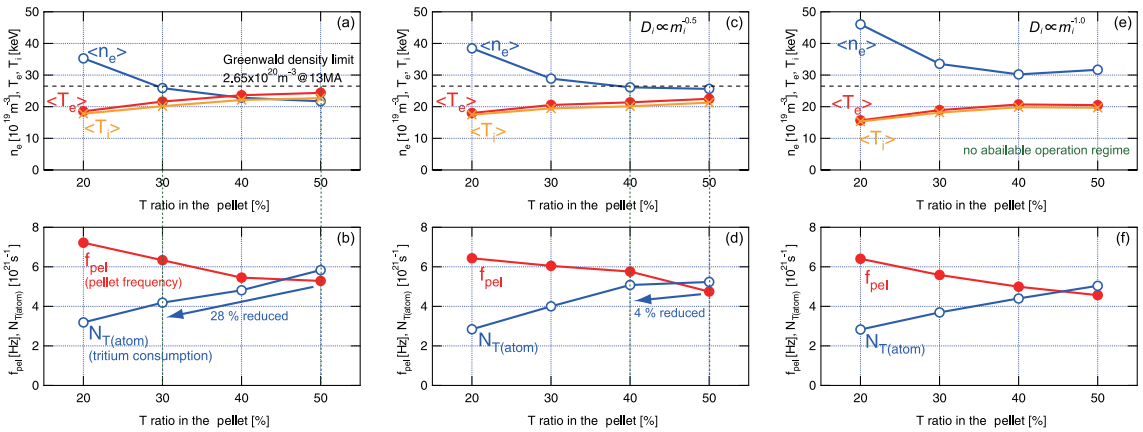

Fig. 4 $<n_e>$, $<T_e>$, $<T_i>$, pellet injection frequency f_{pel} and tritium consumption per unit time $N_{T(atom)}$ plotted against the tritium ratio in the pellet. Dependency of D_i on m_i is not assumed in (a) and (b), and is assumed as $D_i \propto m_i^{-0.5}$ in (c) and (d) and as $D_i \propto m_i^{-1.0}$ in (e) and (f).

4. Conclusion

The relationships between the D/T ratio in the fuel pellet and parameters of the D-T burning plasmas in a tokamak reactor were analyzed numerically using the TOTAL simulation code.

The operation regime of temperature and density depends on the D/T ratio, given the same requirements for fusion output power. This difference results in the variation of the frequency of the pellet injection. The tritium consumption can be evaluated from the pellet frequency and tritium ratio. From this evaluation, we can propose a scenario which reduces tritium consumption. It employs an operation with low-tritium-ratio pellets and higher electron density.

However, if the particle diffusion coefficient of ions and ion mass are negatively correlated, we have to take care that the electron density is increased too much due to the improved confinement of He^{2+} ions. In this case, the tritium reduction scenario stated above tends to be limited by the density limit in cases with a large dependence of the transport on the ion mass. An investigation of the effective exhaust of the He ash will be needed to suppress the increase of electron density and to realize the tritium reduction scenario under the density limit.

We assumed the isotope effect only on the particle transport in the present study. In addition to that, an investigation of the isotope effect on the heat transport is needed. Modeling of the isotope effect that agrees with the experimental data such as the scaling of the energy confinement time should also be explored.

[1] R. J. Hawryluk, J. Plasma Fusion Res. SERIES **5**, 12 (2002).
[2] ITER Physics Expert Groups on Confinement and Transport and Confinement Modelling and Database, Nuclear Fusion **39**, 2175 (1999).
[3] K. Yamazaki and T. Amano, Nucl. Fusion **32**, 633 (1992).
[4] K. Yamazaki *et al.*, Nucl. Fusion **25**, 1543 (1985).
[5] S. P. Hirshman *et al.*, Comput. Phys. Commun. **43**, 143 (1986).
[6] M. Erba *et al.*, Plasma Phys. Control. Fusion **39**, 261 (1997).
[7] Y. B. Kim *et al.*, Phys. Fluids B **3**, 384 (1991).
[8] A. L. Rogister, Nucl. Fusion **41**, 1101 (2001).
[9] Y. Higashiyama *et al.*, Plasma Fusion Res. **3**, S1048 (2008).
[10] T. S. Harm and K. H. Burrell, Phys. Plasmas **2**, 1648 (1995).
[11] F. L. Hinton and G. M. Staebler, Phys. Fluids B **5**, 1281 (1993).
[12] T. Fujita *et al.*, Phys. Rev. Lett. **78**, 2377 (1997).
[13] K. Yamazaki *et al.*, Fusion Eng. Des. **81**, 2743 (2006).
[14] L. R. Bayler *et al.*, Fusion Technol. **34**, 425 (1998).
[15] A. R. Polevoi and M. Shimada, Plasma Phys. Control. Fusion **43**, 1525 (2001).
[16] P. Parks *et al.*, Nucl. Fusion **17**, 539 (1977).